

Contents lists available at ScienceDirect

Organic Geochemistry

journal homepage: www.elsevier.com/locate/orggeochem

Distributions of bacterial and archaeal membrane lipids in surface sediments reflect differences in input and loss of terrestrial organic carbon along a cross-shelf Arctic transect



Ayça Doğrul Selver^a, Robert B. Sparkes^a, Juliane Bischoff^b, Helen M. Talbot^b, Örjan Gustafsson^c, Igor P. Semiletov^{d,e,f}, Oleg V. Dudarev^{e,f}, Stephen Boulton^a, Bart E. van Dongen^{a,*}

^a School of Earth, Atmospheric and Environmental Sciences and Williamson Research Center, University of Manchester, Oxford Road, Manchester M13 9PL, UK

^b School of Civil Engineering and Geosciences, Newcastle University, Newcastle upon Tyne NE1 7RU, UK

^c Department of Applied Environmental Science (ITM) and the Bert Bolin Centre for Climate Research, Stockholm University, Sweden

^d Tomsk Polytechnic University, 30, Lenin Avenue, Tomsk 634050, Russia

^e International Arctic Research Center, University of Alaska, Fairbanks, AK 99775-7340, USA

^f Pacific Oceanological Institute Far Eastern Branch of the Russian Academy of Sciences, Vladivostok 690041, Russia

ARTICLE INFO

Article history:

Received 14 August 2014

Received in revised form 13 November 2014

Accepted 6 January 2015

Available online 22 January 2015

Keywords:

East Siberian Sea

Kolyma River

River–sea transect

Glycerol dialkyl glycerol tetraether

Bacteriohopanepolyols

BIT

 R'_{soil}

ABSTRACT

Enhanced climate warming affecting the Arctic region could have a dramatic impact on the terrigenous organic carbon (terrOC) stored in the Eurasian permafrost and could increase the amount of OC remobilized to the Arctic shelves. An improved understanding of the fate of this remobilized soil OC is essential for better understanding of the consequences for the Arctic and global carbon cycle. In this study, glycerol dialkyl glycerol tetraethers (GDGTs) and bacteriohopanepolyols (BHPs) in surface sediments along a 500 km cross shelf transect from the mouth of the Kolyma River to the middle of the vast East Siberian Sea were analysed to assess their potential and that of the associated branched and isoprenoid tetraether (BIT) and R'_{soil} indices for tracing terrOC in Arctic systems. Both BHP and GDGT contributions indicated the greatest contribution of terrOC close to the river mouth, while the associated indices showed declining trends in an offshore direction, supporting an increasing marine OC input and/or a decrease in terrOC. However, while the BHPs indicated a dominance of terrOC at the start of the transect, the GDGTs suggested a much larger, almost 50%, marine OC input at this point. In addition, the BIT index displayed an exponential decline, controlled mainly by a substantial contribution of marine GDGTs, while R'_{soil} revealed a linear trend governed primarily by the removal of soil marker BHPs.

These field results suggest that both biomarker approaches could be used to trace terrigenous derived OC in the Arctic environment. However, using a single proxy approach is not recommended and may lead to an under or over estimation of the relative importance of terrOC. Using a multi-proxy approach is valuable for fully understanding the fate of terrigenous derived OC along Arctic land-ocean transects.

© 2015 The Authors. Published by Elsevier Ltd. This is an open access article under the CC BY license (<http://creativecommons.org/licenses/by/4.0/>).

1. Introduction

The Arctic terrestrial regions contain approximately half of all global soil organic carbon (OC; [Tarnocai et al., 2009](#)), locked primarily in the first few metres of pan-Arctic permafrost. The widespread extent of the permafrost currently limits the exchange between this large OC reservoir with other more active carbon pools, including the atmosphere. However, since the region is subjected to a warming at 2–3× the global average rate ([Zwiers, 2002](#); [ACIA, 2004](#); [Trenberth et al., 2007](#)), dramatic changes in the release

of terrigenous OC (terrOC) are expected to occur, including an increase in the amount transported to the Arctic shelf seas. There is therefore a requirement to better understand the fate of this remobilized OC on the Arctic shelf ([AMAP, 2012](#); [Vonk and Gustafsson, 2013](#)).

Although it has been widely accepted that, in the marine realm, terrOC is more resistant to degradation than marine OC ([Canuel and Martens, 1996](#); [Hedges and Oades, 1997](#); [van Dongen et al., 2000](#)), recent studies have indicated that a substantial proportion of the fluvially transported terrOC behaves non-conservatively and is degraded close to the point of origin ([van Dongen et al., 2008b](#); [Karlsson et al., 2011](#); [Vonk et al., 2012](#); [Zhu et al., 2013](#); [Tesi et al., 2014](#); [Sánchez-García et al., 2014](#)). Van Dongen et al.

* Corresponding author.

E-mail address: Bart.vandongen@manchester.ac.uk (B.E. van Dongen).

(2008b), for instance, showed that ca. 65% of the terrigenous particulate OC transported by the Kalix River is degraded within 30 km of the river mouth. A comparable proportion is lost annually during mixing in the Laptev and East Siberian seas (Alling et al., 2010; Sánchez-García et al., 2011). In addition, Vonk et al. (2012) determined that ca. 66% of the 44×10^{12} g/yr of OC released by coastal erosion in the East Siberian region is degraded and transported to the atmosphere. High CO₂ flux and CH₄ flux to the atmosphere above the East Siberian Arctic Shelf (Semiletov et al., 2007, 2013; Shakhova and Semiletov, 2007; Anderson et al., 2009; Shakhova et al., 2010, 2014), as well as CO₂ saturated shelf water (Semiletov et al., 2012, 2013), support the idea of more extensive OC degradation in the region than previously thought. Recent analyses indicate that Arctic waters are experiencing widespread ocean acidification (AMAP, 2013). Due to high freshwater and terrOC input, CO₂ neutralization capacity of the Arctic Ocean is low, making the waters more sensitive to ocean acidification (AMAP, 2013). Climate enhanced remobilization and associated decomposition of terrOC may therefore not only cause an increase in the release of greenhouse gases to the atmosphere (Guo et al., 2004, 2007; Gustafsson et al., 2011), resulting in a positive feedback to climate warming, but could also cause further acidification of the Arctic Ocean (Sabine et al., 2004; The Royal Society, 2005) which ultimately alters marine ecosystems.

In order to better understand the rate of loss of the terrOC transported to the Arctic shelf, it is essential to determine the relative importance of marine and terrOC in the Arctic marine environment. This has been done mainly at a bulk level using proxies such as C/N ratio and $\delta^{13}\text{C}$ values of the bulk OC (Fernandes and Sicre, 2000; Guo et al., 2004; Drenzek et al., 2007; Vonk et al., 2008; Semiletov et al., 2012). However, considering that these proxies cannot be used to distinguish between different terrigenous carbon sources, for instance the relative input of soil and plant derived OC, other biomarker based proxies are needed. Recently, the discovery of specific microbial soil biomarkers has resulted in the development of a number of proxies that can be used to trace the terrestrial/soil derived OC along riverine systems (Sinninghe Damsté et al., 2000; Sáenz et al., 2011a; Zhu et al., 2011a, 2013; Doğrul Selver et al., 2012). The first molecularly based proxy is based on glycerol dialkyl glycerol tetraether (GDGT) membrane lipids and has been applied in a variety of settings (e.g. Weijers et al., 2007, 2009, 2011; Doğrul Selver et al., 2012; Huguet et al., 2012; Schouten et al., 2012). Branched GDGTs (br-GDGTs; see Appendix A for structures), produced by anaerobic soil bacteria (Weijers et al., 2007), are found mainly in terrigenous dominated environments (Hopmans et al., 2004; Weijers et al., 2006; Sinninghe Damsté et al., 2009; Tierney and Russell, 2009; Peterse et al., 2011). In contrast, isoprenoid GDGTs (iso-GDGTs), specifically crenarchaeol, are synthesized mainly by marine Thaumarchaeota (Sinninghe Damsté et al., 2002; Schleper et al., 2010) and Euryarchaeota (Lincoln et al., 2014). The GDGT related branched and isoprenoid tetraether (BIT) index (Hopmans et al., 2004) was developed on the basis of these assumptions and has been applied to trace fluvially transported terrOC to marine sediments worldwide (Schouten et al., 2013a).

A second biomarker proxy is based on bacteriohopanepolyols (BHPs), which are pentacyclic triterpenoids with polyfunctionalized side chains (see Appendix A for structures; e.g. Rohmer, 1993). BHPs are synthesized by various bacteria (Ourisson and Rohmer, 1982; Ourisson et al., 1987) and are observed in recent as well as older sediments and soils (van Dongen et al., 2006; Cooke et al., 2008b, 2009; Handley et al., 2010). Some BHPs, such as adenosylhopane and related BHP compounds, have a terrestrial origin and are therefore considered to be 'soil marker' BHPs (Appendix A; Talbot and Farrimond, 2007). On the other hand, bacteriohopanetetrol (BHT), although typically

present in all environments (Talbot et al., 2003; Talbot and Farrimond, 2007; Cooke, 2010; van Winden et al., 2012), is usually the most abundant BHP in marine sediments (Blumenberg et al., 2010; Sáenz et al., 2011b) and is therefore used as a 'pseudo' marine representative end member. Zhu et al. (2011a) used the relative abundance of soil marker BHPs vs. BHT (R_{soil} proxy) to trace the soil input to surface sediments along a Yangtze River–East China Sea transect. Recent research along a sub-Arctic Kalix River–Bothnian Bay transect showed that methylated soil marker BHPs (see Appendix A for structures) had a discontinuous presence throughout the transect. Excluding these methylated soil markers from the R_{soil} calculation (R'_{soil}) resulted in much better correlation with other proxies. Therefore, the R'_{soil} index rather than the R_{soil} proxy is suggested to be used in the (sub-)Arctic region (Doğrul Selver et al., 2012).

Both BHPs and GDGTs have been observed in Arctic shelf sediments (van Dongen et al., 2008a; Cooke et al., 2009; Taylor and Harvey, 2011; Doğrul Selver et al., 2012; De Jonge et al., 2014; Ho et al., 2014), including the East Siberian Arctic Shelf (van Dongen et al., 2008a; Cooke et al., 2009), but the extent to which these lipids can be used to trace a terrigenous contribution to the East Siberian Arctic Shelf remains unclear. The objectives of this study were to determine to what extent GDGT and BHP based proxies can be used for tracing the terrOC contribution in this globally highly important but largely understudied part of the world. To this end, surface sediments along a transect in the East Siberian Sea (ESS) from the mouth of the Kolyma River to the middle of the ESS were analysed. The outcomes of the BHP and GDGT analyses were compared with the results of other bulk proxies used to trace terrigenous contributions ($\delta^{13}\text{C}$ and $\delta^{15}\text{N}$) to determine whether or not molecularly based proxies can be used to trace the various OC sources in the Arctic environment.

2. Methods

2.1. Study area and sample collection

The Kolyma River in northeastern Siberia, with a total catchment area of 647×10^3 km² (Stein and MacDonald, 2004) is the largest Arctic river basin completely underlain by continuous permafrost (Holmes et al., 2011), with active layer depth ranging from 0.2 m in the north to 1 m in the south of the catchment (Uhlířová et al., 2007). Tundra vegetation is the dominant vegetation along the coast, while taiga forests are more dominant in the rest of the basin (Huh et al., 1998). The river has a mean annual water discharge of 114 km³/yr (Cooper et al., 2008), with a peak flow during late May–early June and estimated annual transport of 0.46 Tg dissolved OC and 0.31 Tg of particulate OC (Lobbés et al., 2000).

Eight surface sediment samples were collected along a river mouth-shelf transect tracing the prehistoric path of the Kolyma River ('Kolyma River-ESS transect') in September 2008 during the International Siberian Shelf Study expedition (ISSS-08; Fig. 1; Semiletov and Gustafsson, 2009). They were collected with a dual gravity corer (GEMAX) or, in the case of stations YS-34B and YS-41, a van Veen grab sampler. The sampling station closest to the river mouth, YS-34B (46 km from the mouth), was the only station in an area with a water depth < 20 m (10 m; Table 1). All other stations were situated further off the mouth (100–513 km), with water depth between 31 and 49 m (Table 1). Aliquots of the grab samples were obtained with stainless steel spatulas, transferred to pre-cleaned polyethylene containers and kept frozen until analysis. The cores were sliced into 1 cm sections and processed similarly. Total bulk OC and $\delta^{13}\text{C}$ had been determined previously (Vonk et al., 2010), and ranged from 8–13.6% and -27.3 to -23.9% respectively (Table 1). $\delta^{15}\text{N}$ values were measured on triplicate

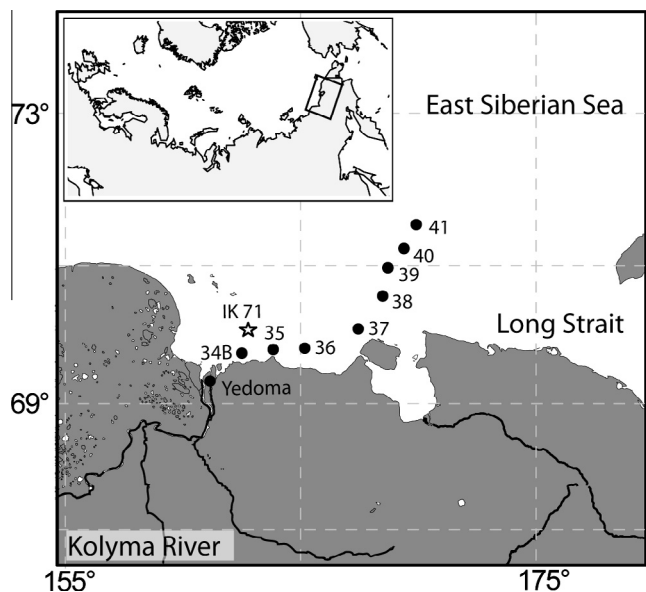


Fig. 1. Map of Kolyma River–ESS transect showing sampling stations (YS-xx; exact locations in Table 1). The star is a reference station IK-71 (van Dongen et al., 2008a).

samples using isotope mass spectrometry (Euro Hydra 20/20; University of California, Davis Stable Isotope Facility, USA) and ranged from 4.2 to 9.3‰.

In addition to the marine sediments, three Yedoma samples, from the Kolyma River catchment area (69.46° N – 161.79° E; Tesi et al., 2014), were analysed to determine the relative amounts of br-GDGTs and crenarchaeol as well as the BHP distribution in this type of sediment. These samples were collected from erosion profiles and represent the composition of terrigenous material transported via coastal erosion.

2.2. Extraction and fractionation

Freeze dried samples were extracted using a modified Bligh-Dyer method as described by Tierney et al. (2012). Briefly, 5 g (dry wt.) were ultrasonically extracted (40 °C for 10 min followed by centrifugation at 2500 rpm for 5 min) with MeOH:dichloromethane (DCM):aqueous phase (2:1:0.8, v/v/v), the aqueous phase consisting of 0.05 M phosphate buffer at pH ca.7.4. The process was repeated 2× using the same solvent mixture and the supernatants were combined. DCM fractions were recovered by addition of phosphate buffer and DCM to the supernatants. The

combined DCM fractions were rotary evaporated to near dryness, transferred to vials using DCM:MeOH (2:1 v/v) and evaporated to dryness under a stream of N₂ to obtain the total lipid extracts which were split into three aliquots.

The first set of aliquots was used for GDGT analysis and separated into core lipid (CL) and intact polar lipid (IPL) fractions using silica column chromatography with 4 ml hexane:EtOAc (1:1, v/v) and 8 ml MeOH, respectively. After separation and the addition of 0.2 µg of a C₄₆ GDGT standard, the CL fraction was dried under a N₂ flow, redissolved in hexane: isopropanol (IPA; 99:1) and filtered through 0.45 µm PTFE filter. Analysis of GDGTs were carried on the CL fraction using the method reported by Hopmans et al. (2004) via high performance liquid chromatography–atmospheric pressure chemical ionisation–mass spectrometry (HPLC–APCI–MS).

The second set of aliquots was used for BHP analysis following a method described by Cooke et al. (2009). Briefly, after addition of the internal standard (5 α -pregnane-3 β ,20 β -diol), each aliquot was acetylated with Ac₂O/pyridine (50 °C for 1 h; stand overnight at room temperature), blown down to dryness using N₂ and redissolved in MeOH:propanol (60:40) for LC–APCI–MSⁿ analysis.

2.3. Instrumental analysis

GDGTs were assigned using an Agilent 1200 HPLC instrument coupled to an Agilent 6130 quadrupole MS instrument equipped with a multimode source operated in APCI positive ion mode using a similar instrumental setup as described by McClymont et al. (2012). The GDGTs were analysed using normal phase LC–MS with a Grace Prevail Cyano HPLC column (3 µm, > 150 mm × 2.1 mm i.d.) and a guard column of the same material. Separation was achieved at 30 °C at 0.2 ml/min and the following gradient profile: 1% IPA in hexane (0–5 min), 1.8% IPA in hexane (at 25 min) and 10% IPA in hexane (at 30 min, held 10 min). Conditions for APCI were: nebulizer pressure 20 psig, vaporiser 250 °C, drying gas (N₂) 6 l/min and 200 °C, capillary voltage 2 kV and corona 5 µA. In order to increase sensitivity/reproducibility, ion scanning was performed in single ion monitoring (SIM) mode using GDGT [M+H]⁺ ions.

Quantification of individual GDGTs was made using a combination of the peak areas of the compounds, the C₄₆ GDGT standard and correction factors for GDGTs. Correction factors were determined on the basis of the peak areas of a synthetic mixture which contains known amounts of br-GDGTs and crenarchaeol with addition of a C₄₆ GDGT standard. The correction factors were applied to minimise the differences in MS response between compounds, allowing determination of individual GDGT concentrations (Schouten et al., 2013b). Previous studies showed that a proportion of CL may carry over into the IPL fraction (Weijers et al., 2011) and

Table 1
Sampling locations, BIT, $\delta^{13}\text{C}$ and R'_{soil} values of surface sediment samples from Kolyma River–ESS transect.

	YS-34B	YS-35	YS-36	YS-37	YS-38	YS-39	YS-40	YS-41
Latitude (N)	69.71	69.82	69.82	70.14	70.70	71.22	71.48	71.97
Longitude (E)	162.69	164.06	166.00	168.01	169.13	169.37	170.55	171.79
Distance from river mouth (km) ^a	46	100	174	258	334	392	443	513
Bottom depth (m)	10	31	32	42	36	44	49	43
Salinity	29.9	30.6	30.8	31.1	31.6	32.4	32.9	33.2
TOC (wt%) ^{b,c}	11.2	12.2	8.0	9.4	10.0	12.3	13.6	13.2
$\delta^{13}\text{C}$ (‰) ^b	−27.3	−26.8	−26.0	−25.7	−25.3	−24.3	−23.9	−23.9
$\delta^{15}\text{N}$ (‰)	4.24	5.90	6.69	7.91	8.17	8.80	9.34	9.34
BIT ^d	0.51	0.28	0.12	0.07	0.05	0.02	0.02	0.03
R'_{soil} ^e	0.57	0.46	0.38	0.30	0.17	0.13	0.08	0.07

^a Distance from 69.65° N–161.50° E.

^b Data from Vonk et al. (2010).

^c Total organic carbon.

^d Branched and isoprenoid tetraether index (Hopmans et al., 2004).

^e (G1 + G2 + G3)/(BHT + G1 + G2 + G3) (compound abbreviations as in Table 2; Doğrul Selver et al., 2012).

a correction may be applied for this. However, this carry over was insignificant, < 2% for all CL factions. In the present study, a correction factor was not applied for this issue but it may be that the GDGT concentrations were up to 2% higher than reported. BIT index values were calculated according to the corrected peak areas of the br-GDGTs and crenarchaeol (Eq. 1).

$$\text{BIT} = (\text{br-GDGT I} + \text{II} + \text{III}) / (\text{br-GDGT I} + \text{II} + \text{III} + \text{crenarchaeol}) \quad (1)$$

Triplicate analysis yielded standard errors of ± 1 to 12 $\mu\text{g/g OC}$ for crenarchaeol and ± 0.1 to 0.8 $\mu\text{g/g OC}$ for br-GDGTs, resulting in a standard error of ± 0 to 0.04 for the BIT index.

Assignment and quantification of BHPs was accomplished using a Surveyor HPLC system (ThermoFinnigan, Hemel Hempstead, UK) equipped with a Gemini C₁₈ column (5 μm , 150 mm \times 3.0 mm i.d.) and a security guard column of the same material (both Phenomenex, Macclesfield, UK). Separation was achieved at 0.5 ml/min at 30 °C with the following gradient: 90% A and 10% B (0 min); 59% A, 1% B and 40% C (at 25 min), then isocratic to 40 min (where A = MeOH, B = water and C = propan-2-ol (all HPLC grade from Fisher Scientific, Loughborough, UK) returning to the starting conditions in 5 min and stabilising for 15 min.

LC-MSⁿ analysis was conducted using a ThermoFinnigan LCQ ion trap mass spectrometer equipped with an APCI source interface operated in positive ion mode. Instrument settings were: capillary 155 °C, APCI vaporiser 400 °C, corona discharge 8 μA , sheath gas flow 40 and auxiliary gas 10 (arbitrary units).

A semi-quantitative estimate of BHPs was calculated from the characteristic base peak ion peak areas of individual BHPs in mass chromatograms relative to the base peak area response of the acetylated 5 α -pregnane-3 β ,20 β -diol internal standard. The reproducibility of a triplicate injection was 3–6% (standard error ± 1 –4 $\mu\text{g/g OC}$) for BHT and 5–8% (standard error: ± 1 –2 $\mu\text{g/g OC}$) for adenosylhopane in the samples, resulting in an absolute standard error of on average ± 0.01 for R'_{soil} . Averaged relative response factors from a suite of five acetylated authentic BHP external standards were used to adjust the peak areas relative to that of the internal standard, where BHPs containing one or more N atoms give an averaged response ca. 12 \times that of the standard and those with no N atoms give a response ca. 8 \times that of the standard (Cooke, 2010; van Winden et al., 2012).

The BHP based R'_{soil} index values were calculated according to the relative concentrations of the soil BHPs adenosylhopane (G1; structure 1e), adenosylhopane type 2 (G2; 1g) and adenosylhopane type 3 (G3; 1g'; Dođrul Selver et al., 2012), respectively and bacteriohopanetetrol (BHT; 1a; Eq. 2).

$$R'_{\text{soil}} = (\text{G1} + \text{G2} + \text{G3}) / (\text{G1} + \text{G2} + \text{G3} + \text{BHT}) \quad (2)$$

3. Results

3.1. GDGT composition

Substantial amounts of br- and iso-GDGTs were observed in all the sediments (Table 2). Along the transect, summed GDGT concentration showed a general increase from 62 $\mu\text{g/g OC}$ in samples from station YS-34B to 1413 $\mu\text{g/g OC}$ in those from station YS-40 (Table 2 and Fig. 2a). With the exception of YS-35, all distributions were dominated by GDGT-0, with a concentration between 25 $\mu\text{g/g OC}$ in the sediment from YS-34B and 774 $\mu\text{g/g OC}$ for YS-40, making up between 38% and 57% of the summed GDGT concentration (Table 2 and Fig. 2a). Besides GDGT-0, a substantial amount of crenarchaeol was also present in all the samples, with a concentration varying between 18 and 597 $\mu\text{g/g OC}$, equivalent to 29–42% of the summed GDGT concentration (Table 2). Crenarchaeol was the most

abundant GDGT at station YS-35. Other iso-GDGTs were also present but in substantially lower amount (upto 26 $\mu\text{g/g OC}$). As well as these iso-GDGTs, br-GDGTs were also present, predominantly br-GDGT II and III, with summed concentration ranging from 6 (YS-39) to 41 $\mu\text{g/g OC}$ (YS-35 and 36) equivalent to 1–31% of the summed GDGTs (Table 2). Minor amounts of br-GDGTs with cyclic units could also be detected in all the sediments, with the exception of YS-34B. BIT index values declined from 0.51 at YS-34B to 0.03 at YS-41, showing a decreasing trend in an offshore direction (Table 1 and Fig. 3a). The summed br-GDGT concentration and crenarchaeol in the Yedoma samples varied between 3.2 and 4.5 $\mu\text{g/g OC}$. and 1.8 and 5.4 $\mu\text{g/g OC}$ respectively (not shown).

3.2. BHP composition

LC-MS analysis showed that up to 16 different BHPs, 6 of which are soil marker BHPs, were present in the Kolyma River–ESS transect sediments (Table 2). The greatest diversity, 16 structures, was in the sediments from YS-34B, 36 and 37, while only 11 structures could be detected in the YS-41 sediment. Total BHP concentration showed a general decrease along the transect from 209 $\mu\text{g/g OC}$ at YS-34B to 138 $\mu\text{g/g OC}$ at YS-41 (Table 2 and Fig. 2b). BHT was the most abundant BHP in all the samples, with a concentration ranging from 64 to 136 $\mu\text{g/g OC}$, constituting 31% to 74% of the summed BHP concentration. Other BHPs in abundance were adenosylhopane (4.1–56 $\mu\text{g/g OC}$), adenosylhopane type II (2.3–28 $\mu\text{g/g OC}$) and aminotriol (5.6–29 $\mu\text{g/g OC}$; Table 2). Although individual concentrations varied, these 3 BHPs constituted between 10% and 43% of the summed BHP concentration (Table 2). Besides BHT and these other three dominant compounds, moderate to minor amounts of other BHPs were also detected, varying between 18% and 35% (Table 2). Summed soil marker BHP (adenosylhopane and adenosylhopane type structures) concentration relatively decreased from 93 $\mu\text{g/g OC}$ at YS-34B to 6.9 $\mu\text{g/g OC}$ at YS-41, equivalent to 44–5% of the summed BHPs concentration (Table 2 and Fig. 2b).

Throughout the transect, R'_{soil} values declined from 0.51 at YS-34B to 0.13 at YS-41, showing a decreasing trend in an offshore direction (Table 1 and Fig. 3a).

The summed soil marker BHP content of the Yedoma samples ranged from 91 to 277 $\mu\text{g/g OC}$ and for BHT from 28 to 62 $\mu\text{g/g OC}$ (data not shown). R'_{soil} values ranged from 0.70 to 0.84. The only other BHPs in Yedoma samples were C-2 methylated BHT and aminotriol, together comprising < 6% of total BHPs in all cases.

4. Discussion

4.1. Origin of nearshore OC

GDGT distributions in the transect were dominated by GDGT 0 and crenarchaeol (> 69% of summed GDGT concentration). Although the lowest relative abundance of these iso-GDGTs was closest to the river mouth it does suggest a substantial marine OC input within 46 km of the mouth (69% of the summed GDGT concentration at YS-34B). The presence of substantial amounts of iso-GDGTs in sediments and suspended particulate matter close to river mouths, indicating a substantial influx of marine derived OC, is not uncommon and has been observed before (Herfort et al., 2006; Kim et al., 2007; Dođrul Selver et al., 2012; Strong et al., 2012). On the other hand, crenarchaeol was also shown to be produced in situ in rivers (Kim et al., 2007; Zell et al., 2013). However, recent analysis of the Kolyma freshet particulate OC yielded very high BIT values (0.99–1) indicating insignificant amounts of fluvially derived crenarchaeol (Peterse et al., 2014). Recent studies of surface sediments from the estuaries of the

Table 2
Concentration of GDGTs and BHPs ($\mu\text{g/g OC}$) and contribution to total GDGTs and BHPs (percent abundance in brackets) in surface sediments from the Kolyma River–ESS transect (BDL, below detection limit).

	Abbreviations	Structure ^a	m/z	YS-34	YS-35	YS-36	YS-37	YS-38	YS-39	YS-40	YS-41
<i>Glycerol dialkyl glycerol tetraethers</i>											
Crenarchaeol			1292	18(29)	95(43)	267(41)	176(39)	388(40)	234(40)	597(42)	354(42)
GDGT 0			1302	25(40)	83(38)	330(51)	248(55)	549(56)	337(57)	774(55)	454(54)
GDGT I			1300	BDL	1.8(1)	9.4(1)	5.8(1)	11(1)	8.4(1)	18(1)	11(1)
GDGT II			1298	BDL	BDL	3.3(0.5)	1.5(0.3)	2.2(0.2)	1.7(0.3)	4.4(0.3)	3.5(0.4)
GDGT III			1296	BDL	BDL	2.0(0.3)	1.1(0.2)	2.4(0.2)	1.4(0.2)	3.5(0.2)	2.1(0.3)
br-GDGT I			1022	4.1(7)	9(4)	10(1)	3.2(0.7)	5.2(0.5)	0.7(0.1)	0.8(0.1)	1.9(0.2)
br-GDGT II			1036	8.8(14)	17(7)	15(2)	4.2(0.9)	8.0(0.8)	1.1(0.2)	3.3(0.2)	3.0(0.4)
br-GDGT III			1050	6.1(10)	11(5)	12(2)	4.9(1)	8.1(0.8)	2.3(0.4)	6.1(0.4)	4.3(0.5)
Σ Cyclic br-GDGTs ^b				BDL	4.2(2)	3.7(0.6)	2.5(0.5)	5.7(0.6)	1.9(0.3)	5.7(0.4)	4.6(0.6)
Σ GDGT				62	221	653	447	980	588	1413	839
<i>Bacteriohopanepolyols</i>											
Bacteriohopanetetrol	D ⁶ BHT	3a	653	3.2(2)	4.8(2)	2.4(2)	5.4(2)	4.3(3)	4.0(2)	3.2(2)	2.7(2)
Bacteriohopanetetrol	BHT	1a	655	64(31)	104(37)	73(49)	136(56)	106(64)	117(71)	113(74)	97(71)
Bacteriohopanetetrol isomer	BHT isomer	1a'	655-II	10(5)	11(4)	9(6)	12(5)	9(6)	10(6)	13(9)	11(8)
Methyl bacteriohopanetetrol	2-Methyl BHT	2a	669	4.3(2)	7.2(3)	3.8(3)	6.1(2)	4.1(2)	4.2(3)	4.8(3)	2.4(2)
Bacteriohopanehexol	BHHexol	1i	771	1.9(0.9)	2.4(0.9)	1.1(0.7)	2.2(0.9)	1.0(0.6)	BDL	BDL	BDL
Aminobacteriohopanetriol	Aminotriol	1b	714	11(5)	29(10)	6.3(4)	10(4)	10(6)	6.3(4)	5.6(4)	11(8)
Aminobacteriohopanetetrol	Aminotetrol	1c	772	1.9(0.9)	5.3(2)	0.7(0.4)	0.8(0.3)	0.9(0.5)	0.3(0.2)	BDL	0.9(0.7)
Aminobacteriohopanepentol	Aminopentol	1d	830	2.9(1)	5.7(2)	0.7(0.5)	0.4(0.2)	0.8(0.5)	BDL	BDL	BDL
Adenosylhopane ^c	G1	1e	746 + 788 + 830 ^d	56(27)	53(19)	23(15)	33(14)	13(8)	10(6)	6.1(4)	4.1(3)
2Me-adenosylhopane ^c	2Me-G1	2e	760 + 802 + 844 ^d	1.4(0.7)	BDL	1.3(0.8)	1.5(0.6)	0.83(0.5)	BDL	BDL	BDL
Adenosylhopane Type 2 ^c	G2	1g	761	23(11)	28(10)	18(12)	20(8)	8.4(5)	5.5(3)	3.4(2)	2.3(2)
2Me-adenosylhopane Type 2 ^c	2Me-G2	2g	775	4.0(2)	4.5(2)	3.4(2)	4.0(2)	1.5(0.9)	1.0(0.6)	BDL	BDL
Adenosylhopane Type 3 ^c	G3	1g'	802	5.8(3)	5.8(2)	3.2(2)	4.2(2)	0.9(0.5)	2.0(1)	0.8(0.5)	0.5(0.4)
2Me-adenosylhopane Type 3 ^c	2Me-G3	2g'	816	2.3(1)	2.4(0.8)	1.3(0.9)	1.9(0.8)	BDL	1.2(0.7)	BDL	BDL
Bacteriohopanetetrol cyclitol ether	BHT cyclitol ether	1f	1002 + 1044 ^e	15(7)	17(6)	2.4(2)	3.9(2)	3.0(2)	2.4(1)	2.1(1)	4.9(4)
Bacteriohopanetetrol glucosamine	BHT glucosamine	1h	1002	1.3(0.6)	1.5(0.5)	0.7(0.5)	1.0(0.4)	1.1(0.7)	0.9(0.5)	1.1(0.7)	0.8(0.6)
Σ BHPs				209	281	150	244	164	166	154	138

^a See Appendix A.

^b Summed concentrations of br-GDGT Ib, Ic and IIb, IIc.

^c Soil marker BHPs.

^d Diacetate, triacetate and tetraacetate, respectively.

^e Heptaacetate and octaacetate.

Kalix River (Sweden; Doğrul Selver et al., 2012) and the Yangtze River (China; Zhu et al., 2011b), for instance, also indicated the presence of a significant amount of crenarchaeol close to the river mouths.

The presence of substantial amounts of br-GDGTs (both with and without cyclic units) in the sediments suggests a substantial influx of terrOC. Br-GDGTs are abundantly produced in soils and peats (Weijers et al., 2006) and accepted to be transported predominantly to the marine environment by rivers and erosion (Hopmans et al., 2004). Indeed Peterse et al. (2014) recently showed that the br-GDGTs in Kolyma River suspended particulate matter and lake surface sediments in the Kolyma River catchment were derived mainly from (surface) soils, either indirectly delivered by the river, or directly through thawing. However, Peterse et al. (2014) also showed that additional br-GDGT production may take place in lakes/streams. These results are in line with other studies from (non-)Arctic regions (Zell et al., 2013; De Jonge et al., 2014) suggesting a mixed origin of the br-GDGTs observed along the transect. Furthermore, minor production of br-GDGTs both in marine sediments and in marine suspended particulate matter (Peterse et al., 2014; Zell et al., 2014) cannot be excluded. However, this would not affect the observed BIT values considering the substantial increase in crenarchaeol in this region.

The Yedoma samples from the Kolyma River catchment area contained relatively low amounts of br-GDGTs, between 3.2 and 4.5 $\mu\text{g/g OC}$ for those analysed here and 9.2 $\mu\text{g/g OC}$ for the sample analysed by Peterse et al. (2014). Considering that there is a substantial presence of crenarchaeol in these Yedoma samples, unlike other terrigenous samples in the catchment (Peterse et al., 2014) this resulted in widely varying BIT values (0.4–0.8). The exact origin of the relatively high crenarchaeol contribution remains

unclear. The br-GDGT concentration values are 4–12 \times lower than those in the surface sediments taken at the stations closest to the river mouth (YS-34B and YS-35; 19–37 $\mu\text{g/g OC}$ Table 2) or up to 90 \times lower than those in lake surface sediments from the Kolyma catchment (284 $\mu\text{g/g OC}$; Peterse et al., 2014), indicating that the contribution of Yedoma coastal erosion is minimal. Combined, these observations suggest that the majority of the br-GDGTs in the Kolyma estuary sediments originated from thawing (surface) soils and in situ production in the Kolyma River.

The presence of a substantial amount of br-GDGTs and iso-GDGTs is reflected in the BIT index and resulted in a value of 0.51 for the YS-34B sediment. In line with previous studies (Smith et al., 2010; Doğrul Selver et al., 2012), the reduction in BIT values offshore is most likely due to a combination of both removal of the terrOC by the time it reaches 46 km from the river mouth and a substantial influx of marine derived OC. In contrast, previous GDGT analysis of a sediment taken near YS-34B (station IK-71; Fig. 1) showed much higher relative br-GDGT abundance compared with crenarchaeol (van Dongen et al., 2008a). This resulted in a much higher BIT index value (0.91), suggesting a much higher dominance of terrOC. However, in that study no internal standard was used and correction factors were not applied. Schouten et al. (2013b) recently showed that this could cause a positive bias in calculation of concentrations and BIT index values. Applying the same uncorrected data analysis technique to YS-34B yields a similar BIT value (0.87), indicating that the composition at both stations is actually comparable. Given that Peterse et al. (2014) report BIT values of 0.99–1 for the Kolyma River, and we have measured BIT values of 0.02 by station YS-39, a simple end member calculation suggests that only ca. 50% of the OC in the sediment is of terrigenous origin. However, given that GDGT

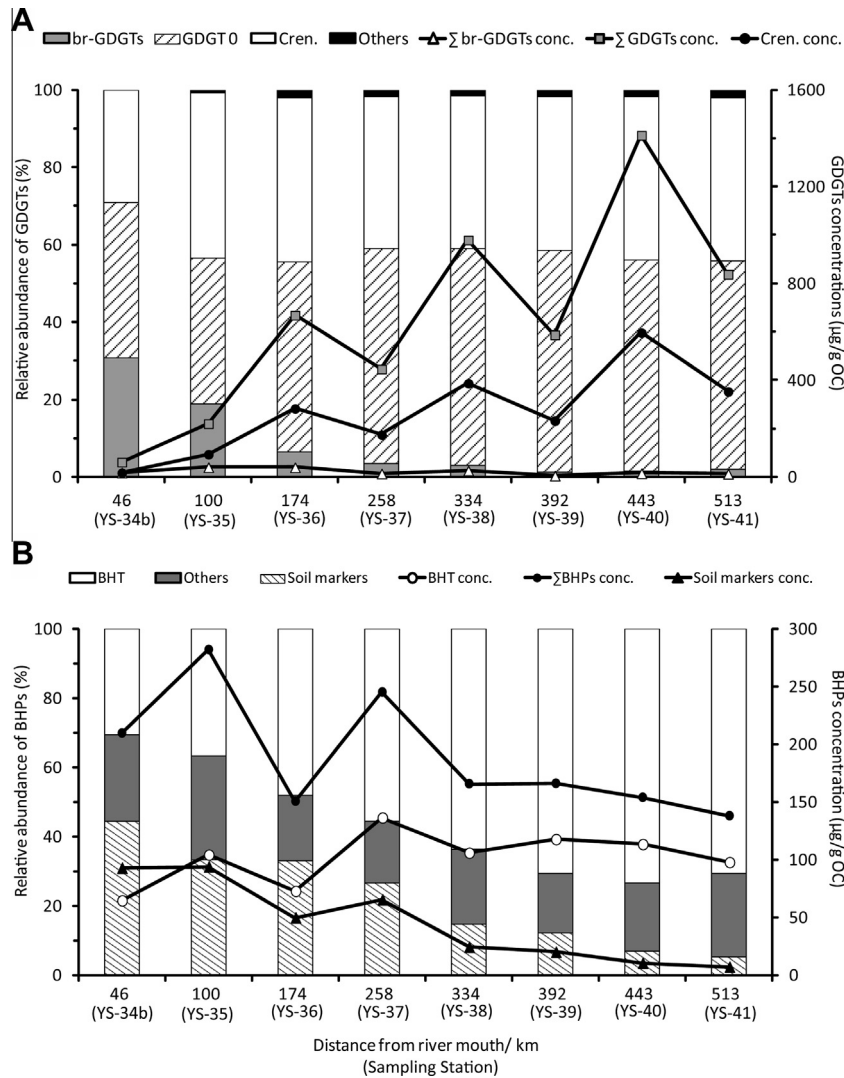


Fig. 2. Histograms of relative abundance and concentration ($\mu\text{g/g OC}$) of (A) GDGTs and (B) BHPs in the Kolyma River–ESS transect surface sediments.

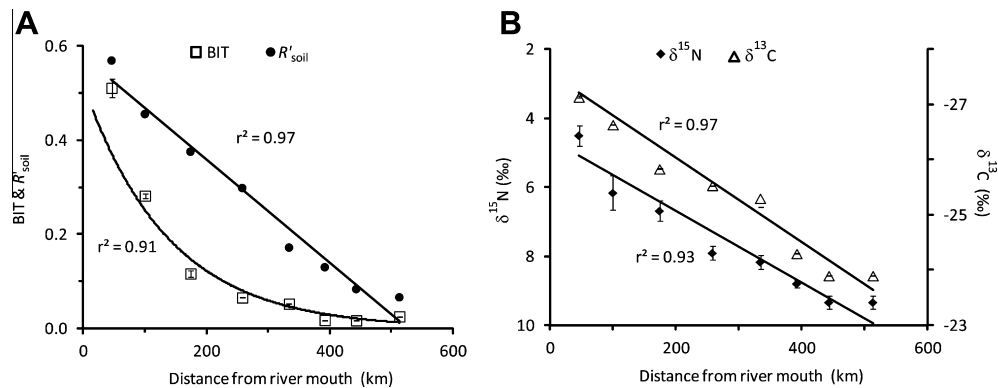


Fig. 3. Plots of (A) BIT and R'_{soil} and (B) $\delta^{13}\text{C}$ (data from Vonk et al., 2010) and $\delta^{15}\text{N}$ vs. distance from Kolyma River mouth.

concentrations in Yedoma are particularly low, the influx of coastal erosion-derived sediment is likely not considered in this simple calculation, and the 50% estimate for terrigenous sediment is probably too low – this is discussed below.

The substantial influx of marine derived OC, as suggested by the GDGT analysis, is not supported by other studies of the same sediment (Vonk et al., 2010, 2012; Tesi et al., 2014). The depleted $\delta^{13}\text{C}$

value (-27.3‰ ; Vonk et al., 2010), the high concentration of high molecular weight (HMW) *n*-alkanes ($1170 \mu\text{g/g OC}$; Vonk et al., 2010) and the substantial amount of lignin present (28 mg/g OC ; Tesi et al., 2014) together suggest a much higher dominance of terrigenous OM. Indeed, a dual carbon isotopic mixing model, based on both bulk ^{13}C and ^{14}C analyses, suggested a much higher terrOC contribution (ca. 85%; Vonk et al., 2012) if compared with

the GDGT based estimation. In addition, the BHP results also suggest a much lower influx of marine OC. Soils usually have a wide BHP diversity (Cooke et al., 2008a; Xu et al., 2009; Zhu et al., 2011a), relative to sediments or suspended matter from marine dominated areas. Sáenz et al. (2011a), for instance, found 8 BHPs in estuarine suspended particulate matter and only 1 BHP in open ocean samples from a river–ocean transect off the Pacific coast of Panama. In line with other sediments from river catchments (Zhu et al., 2011a; Doğrul Selver et al., 2012) the BHPs in the sediment from YS-34B had a wide diversity (Table 2 and Fig. 2b); 16 different BHPs were present, 6 of which are soil marker BHPs, suggesting a predominantly terrigenous origin. In addition, the BHP composition at YS-34B was in line with previous analysis of the sediment from IK-71 (Cooke et al., 2009), which showed 13 different BHPs.

In addition to the relative composition, the relatively high abundance of soil marker BHPs (44% of total BHPs) at YS-34B supports the inference of a high terrigenous influx. The abundance in the sediments is high compared with the relative contribution of soil marker BHPs generally observed in soils worldwide (avg. 28%; Cooke et al., 2009; Cooke, 2010); however, the values for the 3 Yedoma samples are even higher (69–82%). Such high values are consistent with permafrost soil profiles from Svalbard in the Arctic region for instance, which showed up to 75% (avg. 49%, excluding surface organic mat layers) of the total BHPs as soil marker BHPs (Rethemeyer et al., 2010). The dominance of soil (terrigenous) derived BHPs is clearly reflected in the R'_{soil} index, resulting in a value of 0.57 for the YS-34B sediment, and is slightly higher than the R'_{soil} index (0.44) calculated from the BHP concentration at IK-71 (Cooke et al., 2009). The average R'_{soil} values for the 3 Yedoma samples is 0.76, suggesting that as much as 75% of the OC in the sediment from YS-34B is of terrigenous origin; however, as BHP terrigenous end member data for this region are currently limited to 3 samples from one profile, this estimate remains tentative. The proportion is comparable with the outcome of a dual carbon isotopic mixing model (Vonk et al., 2012) and lignin analysis (Tesi et al., 2014) for the same sediment, supporting the hypothesis that most of the terrOC is not degraded/removed during the first 46 km of transport off the river mouth.

To summarise, $\delta^{13}\text{C}$ (Vonk et al., 2010), BHP composition and R'_{soil} index (this study), lignin and other terrestrial lipid data (Vonk et al., 2010; Tesi et al., 2014) and the outcome of a dual carbon isotopic mixing model using ^{13}C and ^{14}C (Vonk et al., 2012) all indicate that the OM transported to the sediment at station YS-34B, the start of the transect, is heavily dominated by terrigenous OC. However, the GDGT results seem to contradict this, suggesting a much lower terrOC derived dominance. To explore this discrepancy the trends along the Kolyma River–ESS transect are discussed in more detail below.

4.2. OC input and removal along the transect

Besides a dominance of terrOC at YS-34B, previous studies indicated, from lipid and isotope analysis of suspended particulate matter and surface sediments, an increasing marine derived OC contribution along the Kolyma River–ESS transect (Vonk et al., 2010, 2012). For instance, the declining HMW/LMW *n*-alkane ratio (from 51.2 to 19), enriching $\delta^{13}\text{C}$ (from -27.3‰ to -23.9‰) and $\delta^{15}\text{N}$ values (from 4.2–9.3‰; Vonk et al., 2010) indicate an increasing addition of marine-derived OC in an offshore direction. In addition, using a 3 end member mixing model that included bulk radiocarbon age and $\delta^{13}\text{C}$ data, Vonk et al. (2010) observed an increasing marine, a decreasing riverine and a constant coastal erosion OC contribution with increasing distance from the river mouth.

Along the transect, the diversity of BHPs decreased from 16 components (at YS-34B) to 11 (at YS-41), due mainly to loss of

methylated soil markers, BHHexol and Aminopentol (Table 2). Earlier studies showed a similar declining trend in BHP diversity across other land–sea transects, including a Kalix River–Bothnian Bay transect (Doğrul Selver et al., 2012), a Yangtze River–East China Sea transect (Zhu et al., 2011b) and a river–ocean transect off the Pacific coast of Panama (Sáenz et al., 2011a). The particular loss of methylated soil markers is typical and has been observed previously, such as along the Kalix River–Bothnian Bay transect (Doğrul Selver et al., 2012).

As well as the reduction in BHP diversity, an increasing contribution of crenarchaeol (from 18–354 $\mu\text{g/g}$ OC) as well as decreasing br-GDGTs (from 19–14 $\mu\text{g/g}$ OC) and soil marker BHP contribution (from 93–6.9 $\mu\text{g/g}$ OC) could also be observed along the same transect (Fig. 2 and Table 2). The changes are well reflected in the BIT and R'_{soil} indices and reveal declining trends (from 0.51–0.02 and from 0.57–0.07, respectively) throughout the transect. In line with previous studies for other river–ocean transects (Smith et al., 2010; Zhu et al., 2011a; Doğrul Selver et al., 2012) this further suggests a shift to a more marine-dominated environment in an offshore direction.

Although all proxies suggest a general shift towards a more marine dominated environment, a remarkable difference could be observed in the behaviour of the BIT index vs. the other indices. The bulk proxies ($\delta^{13}\text{C}$ and $\delta^{15}\text{N}$) and the R'_{soil} index revealed a clear linear decreasing trend with distance from the river mouth, with r^2 values between 0.91 and 0.97 ($n = 8$, $p < 0.05$, Fig. 3). In contrast, the BIT index showed an exponentially decreasing trend ($r^2 = 0.91$; $n = 8$, $p < 0.05$; Fig. 3). In addition, when plotted against each other, strong linear correlations were observed between the R'_{soil} index, $\delta^{13}\text{C}$ and $\delta^{15}\text{N}$ (r^2 between 0.93 and 0.97, $n = 8$, $p < 0.05$; Fig. 4B, C and F). Similarly, BIT also correlates strongly with R'_{soil} , $\delta^{13}\text{C}$ and $\delta^{15}\text{N}$ (r^2 between 0.95 and 0.97, $n = 8$, $p < 0.05$; Fig. 4A, D and E) but only if an exponential correlation is applied. Previous studies showed that the BIT index correlated linearly with $\delta^{13}\text{C}$ as well as with R'_{soil} (Zhu et al., 2011a; Doğrul Selver et al., 2012; Smith et al., 2012). Smith et al. (2010) attributed the correlation between the BIT index and $\delta^{13}\text{C}$ to the geographical conditions (i.e. forested catchment area, steep fjord slopes and high annual rainfall), which resulted in enhanced input of soil derived OC. The difference in behaviour between the BIT index and the bulk indices could be caused by an influx of a substantial amount of resistant plant derived OC, such as lignin derived OC. Previous studies have showed that the BIT index shows only a weak correlation with lignin phenol proxies (Walsh et al., 2008; Smith et al., 2010). Consequently, in systems with a dominant soil OC input, such as Fiordland, New Zealand, the BIT index correlated strongly with $\delta^{13}\text{C}$ (Smith et al., 2010), while in systems with a low soil input but high input of plant derived OC, such as the Vancouver Island Fjords, no significant correlation between BIT and $\delta^{13}\text{C}$ was observed (Walsh et al., 2008). However, such an influx would not only have an effect on the correlation between BIT and $\delta^{13}\text{C}$ along the transect, but also should have a comparable effect on the correlation between R'_{soil} and $\delta^{13}\text{C}$. The absence of such an effect indicates that a substantial influx of resistant plant derived OC is not likely the major cause of the difference in trends observed.

Another possible cause is the difference in the removal of br-GDGTs, soil marker BHPs and other terrestrial derived OC throughout the transect. This can be attributed to a difference in susceptibility to degradation of the different compound classes, although Tesi et al. (2014) recently showed that sediment sorting could also play an important factor. Lignin phenols, for instance, are removed more rapidly than wax lipids in the Arctic environment. Lignin tends to be adsorbed on larger particles, becoming part of the heavier fraction in the water column and transported to surface sediments much closer to the river mouths than wax lipids, which are adsorbed mainly on finer (lighter) particles. It

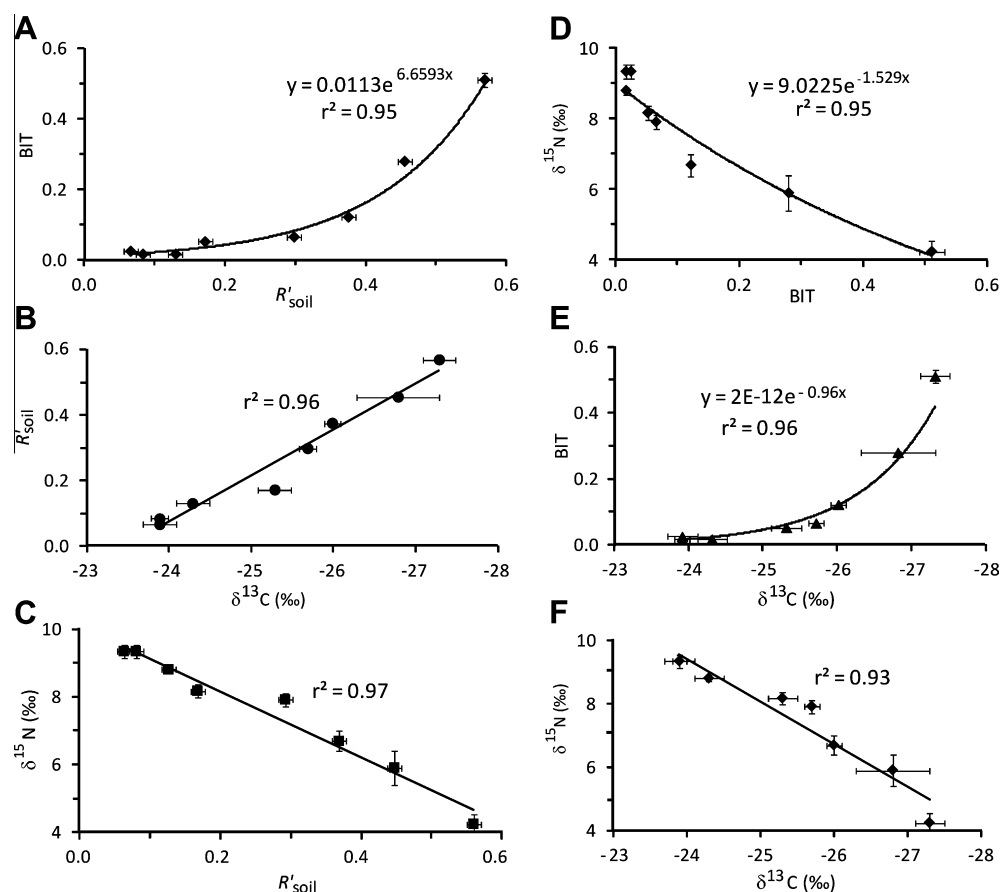


Fig. 4. Plots of R'_{soil} index vs. (A) BIT, (B) $\delta^{13}\text{C}$ (data from Vonk et al., 2010) and (C) $\delta^{15}\text{N}$, (D) $\delta^{15}\text{N}$ vs. BIT, (E) BIT vs. $\delta^{13}\text{C}$ and (F) $\delta^{15}\text{N}$ vs. $\delta^{13}\text{C}$ in surface sediments of the Kolyma River–ESS transect.

remains unclear whether sediment sorting also plays an important role in the case of GDGTs or BHPs, but comparable analyses of the Madeira Abyssal Plain suggest this is likely (Huguet et al., 2008). More importantly, soil marker BHPs appear to be removed more rapidly than br-GDGTs (6 fold vs. 2 fold decrease in concentration in an offshore direction, respectively; Appendix B), in line with a study of a Yangtze River–East China Sea transect (Zhu et al., 2013). Therefore this moderate decline in br-GDGTs, and thus degradation and/or sediment sorting, cannot completely explain the exponential behaviour of the BIT index.

Another possible explanation is based on the most striking differences in the addition of the (pseudo)marine components crenarchaeol and BHT. Although values vary between the stations, possibly due to influx from the Long Strait, a general substantial crenarchaeol input was observed relative to a considerably lower pseudo marine end member BHT input (24× vs. 2× increase offshore, respectively). Combining these with the relative removal rates of the terrestrial component, as discussed above, suggests that the relatively greater soil marker BHPs removal was not compensated for by the addition of BHT. In contrast, lesser br-GDGT removal was overwhelmed by significant crenarchaeol addition, possibly causing the exponential decrease in the BIT index. In addition, assuming that the influx of crenarchaeol is extremely high in the area, particularly in comparison with the transport of other marine derived OC to the sediments, this would also explain the trends observed between the BIT and the bulk indices.

Given the predominance of coastal erosion in this part of the ESS (Semiletov et al., 2012; Vonk et al., 2012), which may account for the majority of the bulk $\delta^{13}\text{C}$ signal, it is likely that the trends are caused partly by contributions from the different terrestrial

end members, e.g. fluvial vs. coastal erosion. The strong correlation between R'_{soil} , $\delta^{13}\text{C}$ and $\delta^{15}\text{N}$, suggests that, in contrast to the br-GDGTs which, as discussed above originated predominantly from thawing soils and in situ production in the Kolyma River, the major source of BHPs in the marine system may be coastal erosion rather than fluvial transport, as indicated by their significantly higher concentration in Yedoma than the br-GDGTs. This could also explain why these differences are not observed in other (sub-)Arctic systems such as the Kalix River Bothnian Bay transect (Doğrul Selver et al., 2012), where coastal erosion plays a less dominant role. However, to fully understand and quantify the origin/contribution of the specific compound classes on the Arctic Shelf, reliable end member values are needed from various terrestrial environments, including lakes, rivers, ice complex, peat, loess and (top)soils. Furthermore, a more comprehensive assessment of bulk and compound specific data from distal marine settings is required.

4.3. Implications for carbon cycling

From the above discussion, it is clear that all the indices support previous studies (Vonk et al., 2010, 2012; Tesi et al., 2014), showing a reduction in the influx of terrigenous OC in surface sediments along the Kolyma River–ESS transect. Likewise, soil marker BHPs and br-GDGTs show similar declining trends but the magnitude of the reduction is different. Consequently, the BIT index decreases more rapidly than the R'_{soil} index offshore, in contrast to measurements elsewhere (Zhu et al., 2013). The apparent paradox can be resolved by understanding the factors that control both indices. Since the relatively great loss of soil marker BHPs was not

compensated for by the increase in BHT (Appendix B), R'_{soil} is controlled mainly by the removal of soil marker BHPs. On the other hand, due to a significantly high input of crenarchaeol vs. minor decrease in br-GDGTs, the BIT index appears to be controlled primarily by the addition of crenarchaeol. Thus, these two proxies provide complementary insights into the offshore processes.

These field results suggest that both biomarker approaches could be used to trace soil derived OC in the Arctic environment. However, in line with previous studies, using only a single proxy may give an incomplete characterisation of the system and could lead to an under or over estimation of the relative importance of the different contributions. Using a multi-proxy approach is valuable for deducing the relative inputs of marine and terrestrial OC and, combined with the results of previous studies of the same sediments (Vonk et al., 2010; Tesi et al., 2014) has generated a stronger understanding of the processes acting along the Kolyma River–ESS transect. Therefore, this study highlights the importance of combining different proxies to better understand the fate of terrestrially derived OM in the marine environment.

If such a multi-proxy approach were to be applied to other parts of the Arctic region, such as the whole East Siberian Arctic shelf, it could provide a better understanding of the fate of the terrOC exported to the Arctic shelf seas. This would include effects of ocean acidification and the exchange with other more active carbon pools, including the atmosphere.

5. Conclusions

The highest total BHP concentration and widest BHP diversity were observed at the station closest to the river mouth, indicating high terrestrial input at the start of the transect. Along with a drop in diversity and in total BHP concentration, soil marker BHP concentration declined offshore, suggesting a shift to a more marine dominated system.

Conversely, the lowest total GDGT concentration was at the start of the transect, with iso-GDGTs comprising almost 50% of the total GDGTs. This suggests that, unlike the BHPs results, there was an almost equal contribution of marine and terrOC at the start of the transect, relatively close to the river mouth. Total GDGT concentration showed an increase in an offshore direction, due mainly to the input of iso-GDGTs, whereas the br-GDGT contribution dropped along the transect. Taken together, these trends in GDGTs suggest a removal of br-GDGTs and a shift towards a more marine dominated system in an offshore direction.

Both bulk ($\delta^{13}\text{C}$ and $\delta^{15}\text{N}$) and molecularly based indices (BIT and R'_{soil}) declined in an offshore direction, supporting an increasing marine OC input. However a prominent difference was observed in the behaviour of the BIT index vs. the other indices. BIT showed an exponential decline, while all the other indices revealed linear trends throughout the transect. This behaviour of the BIT index is controlled mainly by the substantial addition of crenarchaeol, while R'_{soil} is governed primarily by the removal of soil marker BHPs.

These field results suggest that both biomarker approaches can be used to trace soil derived OC in the Arctic environment. However, in line with previous work, this study has highlighted that using a single proxy approach to trace terrOC in the Arctic environment may lead to an under or over estimation of the relative importance of the different contributions. Using a multi-proxy approach is valuable for deducing the relative inputs of marine and terrestrial OC and leads to a better understanding of the processes acting along land-ocean transects in the Arctic region.

Acknowledgements

We gratefully acknowledge receipt of a NERC research Grant (NE/I024798/1 and NE/I027967/1) to B.E.v.D. and H.M.T., a Ph.D.

studentship to A.D.S. funded by the Ministry of National Education of Turkey, financial support as an Academy Research Fellow to Ö.G. from the Swedish Royal Academy of Sciences through a grant from the Knut and Alice Wallenberg Foundation and support from the Government of the Russian Federation (Grant #2013-220-04-157) to I.S. and O.D. We thank the crew and personnel of the R/V Yakob Smirnitskiy and all colleagues in the International Siberian Shelf Study (ISSS) Program for support, including sampling. We thank P. Lythgoe (University of Manchester) and F. Sidgwick (Newcastle University) for invaluable assistance with LC–MS, T. Tesi for providing the Yedoma samples for the Kolyma catchment area and the Science Research Infrastructure Fund (SRIF) From HEFCE for the ThermoFinnigan LCQ ion trap mass spectrometer (Newcastle University). The ISSS program, is supported by the Knut and Alice Wallenberg Foundation, the Far Eastern Branch of the Russian Academy of Sciences, the Swedish Research Council, the US National Oceanic and Atmospheric Administration, the Russian Foundation of Basic Research, the Swedish Polar Research Secretariat, the Nordic Council of Ministers and the US National Science Foundation. Finally, we thank two anonymous reviewers for constructive suggestions.

Appendix A. Supplementary data

Supplementary data associated with this article can be found, in the online version, at <http://dx.doi.org/10.1016/j.orggeochem.2015.01.005>.

Associate Editor—E.A. Canuel

References

- ACIA, 2004. Impacts of a Warming Arctic: Arctic Climate Impact Assessment. Cambridge University Press, Cambridge, UK.
- Alling, V., Sanchez-Garcia, L., Porcelli, D., Pugach, S., Vonk, J.E., van Dongen, B., Mörth, C.-M., Anderson, L.G., Sokolov, A., Andersson, P., Humborg, C., Semiletov, I., Gustafsson, Ö., 2010. Nonconservative behavior of dissolved organic carbon across the Laptev and East Siberian seas. *Global Biogeochemical Cycles* 24, GB4033. <http://dx.doi.org/10.1029/2010gb003834>.
- AMAP, 2012. Arctic climate issues 2011: changes in arctic snow, water, ice and permafrost. SWIPA 2011 Overview Report. Arctic Monitoring and Assessment Programme (AMAP), Oslo, Norway, xi + 97 pp.
- AMAP, 2013. AMAP Assessment 2013: Arctic Ocean Acidification. Arctic Monitoring and Assessment Programme (AMAP), Oslo, Norway viii + 99 pp.
- Anderson, L.G., Jutterström, S., Hjalmarsson, S., Wählström, I., Semiletov, I.P., 2009. Out-gassing of CO_2 from Siberian Shelf seas by terrestrial organic matter decomposition. *Geophysical Research Letters* 36, L20601.
- Blumenberg, M., Mollenhauer, G., Zabel, M., Reimer, A., Thiel, V., 2010. Decoupling of bio- and geohopanoids in sediments of the Benguela Upwelling System (BUS). *Organic Geochemistry* 41, 1119–1129.
- Canuel, E.A., Martens, C.S., 1996. Reactivity of recently deposited organic matter: degradation of lipid compounds near the sediment–water interface. *Geochimica et Cosmochimica Acta* 60, 1793–1806.
- Cooke, M.P., Talbot, H.M., Farrimond, P., 2008a. Bacterial populations recorded in bacteriohopanepolyol distributions in soils from Northern England. *Organic Geochemistry* 39, 1347–1358.
- Cooke, M.P., Talbot, H.M., Wagner, T., 2008b. Tracking soil organic carbon transport to continental margin sediments using soil-specific hopanoid biomarkers: a case study from the Congo fan (ODP site 1075). *Organic Geochemistry* 39, 965–971.
- Cooke, M.P., van Dongen, B.E., Talbot, H.M., Semiletov, I., Shakhova, N., Guo, L., Gustafsson, Ö., 2009. Bacteriohopanepolyol biomarker composition of organic matter exported to the Arctic Ocean by seven of the major Arctic rivers. *Organic Geochemistry* 40, 1151–1159.
- Cooke, M.P., 2010. The Role of Bacteriohopanepolyols as Biomarkers for Soil Bacterial Communities and Soil Derived Organic Matter. Ph.D. thesis, Newcastle University, Newcastle upon Tyne, UK.
- Cooper, L.W., McClelland, J.W., Holmes, R.M., Raymond, P.A., Gibson, J.J., Guay, C.K., Peterson, B.J., 2008. Flow-weighted values of runoff tracers ($\delta^{18}\text{O}$, DOC, Ba, alkalinity) from the six largest Arctic rivers. *Geophysical Research Letters* 35.
- De Jonge, C., Stadnitskaia, A., Hopmans, E.C., Cherkashov, G., Fedotov, A., Sinnighe Damsté, J.S., 2014. In situ produced branched glycerol dialkyl glycerol tetraethers in suspended particulate matter from the Yenisei River, Eastern Siberia. *Geochimica et Cosmochimica Acta* 125, 476–491.

- Doğrul Selver, A., Talbot, H.M., Gustafsson, Ö., Boulton, S., van Dongen, B.E., 2012. Soil organic matter transport along an sub-Arctic river–sea transect. *Organic Geochemistry* 51, 63–72.
- Drenzek, N.J., Montluçon, D.B., Yunker, M.B., Macdonald, R.W., Eglinton, T.I., 2007. Constraints on the origin of sedimentary organic carbon in the Beaufort Sea from coupled molecular ^{13}C and ^{14}C measurements. *Marine Chemistry* 103, 146–162.
- Fernandes, M.B., Sicre, M.A., 2000. The importance of terrestrial organic carbon inputs on Kara Sea shelves as revealed by *n*-alkanes, OC and $\delta^{13}\text{C}$ values. *Organic Geochemistry* 31, 363–374.
- Guo, L., Semiletov, I., Gustafsson, Ö., Ingri, J., Andersson, P., Dudarev, O., White, D., 2004. Characterization of Siberian Arctic coastal sediments: implications for terrestrial organic carbon export. *Global Biogeochemical Cycles* 18, GB1036.
- Guo, L., Ping, C.-L., Macdonald, R.W., 2007. Mobilization pathways of organic carbon from permafrost to Arctic rivers in a changing climate. *Geophysical Research Letters* 34, L13603.
- Gustafsson, Ö., van Dongen, B.E., Vonk, J.E., Dudarev, O.V., Semiletov, I.P., 2011. Widespread release of old carbon across the Siberian Arctic echoed by its large rivers. *Biogeochemistry* 8, 1737–1743.
- Handley, L., Talbot, H.M., Cooke, M.P., Anderson, K.E., Wagner, T., 2010. Bacteriohopanepolyols as tracers for continental and marine organic matter supply and phases of enhanced nitrogen cycling on the late Quaternary Congo deep sea fan. *Organic Geochemistry* 41, 910–914.
- Hedges, J.L., Oades, J.M., 1997. Comparative organic geochemistry of soils and marine sediments. *Organic Geochemistry* 27, 319–361.
- Herfort, L., Schouten, S., Boon, J.P., Woltering, M., Baas, M., Weijers, J.W.H., Sinninghe Damsté, J.S., 2006. Characterization of transport and deposition of terrestrial organic matter in the Southern North Sea using the BIT index. *Limnology and Oceanography* 51, 2196–2205.
- Ho, S.L., Mollenhauer, G., Fietz, S., Martínez-García, A., Lamy, F., Rueda, G., Schipper, K., Méheust, M., Rosell-Melé, A., Stein, R., Tiedemann, R., 2014. Appraisal of TEX_{86} and TEX_{86} thermometries in subpolar and polar regions. *Geochimica et Cosmochimica Acta* 131, 213–226.
- Holmes, R., McClelland, J., Peterson, B., Tank, S., Buliygina, E., Eglinton, T., Gordeev, V., Gurtovaya, T., Raymond, P., Repeta, D., Staples, R., Striegl, R., Zhulidov, A., Zimov, S., 2011. Seasonal and annual fluxes of nutrients and organic matter from large rivers to the Arctic Ocean and surrounding seas. *Estuaries and Coasts* 35, 369–382.
- Hopmans, E.C., Weijers, J.W.H., Schefuß, E., Herfort, L., Sinninghe Damsté, J.S., Schouten, S., 2004. A novel proxy for terrestrial organic matter in sediments based on branched and isoprenoid tetraether lipids. *Earth and Planetary Science Letters* 224, 107–116.
- Huguet, A., de Lange, G.J., Gustafsson, Ö., Middelburg, J.J., Sinninghe Damsté, J.S., Schouten, S., 2008. Selective preservation of soil organic matter in oxidized marine sediments (Madeira Abyssal Plain). *Geochimica et Cosmochimica Acta* 72, 6061–6068.
- Huguet, A., Wiesenberg, G.L.B., Gocke, M., Fosse, C., Derenne, S., 2012. Branched tetraether membrane lipids associated with rhizoliths in loess: Rhizomicrobial overprinting of initial biomarker record. *Organic Geochemistry* 43, 12–19.
- Huh, Y., Panteleyev, G., Babich, D., Zaitsev, A., Edmond, J., 1998. The fluvial geochemistry of the rivers of Eastern Siberia: II. Tributaries of the Lena, Omoloy, Yana, Indigirka, Kolyma, and Anadyr draining the collisional/accretionary zone of the Verkhoyansk and Cherskiy ranges. *Geochimica et Cosmochimica Acta* 62, 2053–2075.
- Karlsson, E.S., Charkin, A., Dudarev, O.V., Semiletov, I.P., Vonk, J.E., Sánchez-García, L., Andersson, A., Gustafsson, Ö., 2011. Carbon isotopes and lipid biomarker investigation of sources, transport and degradation of terrestrial organic matter in the Buor-Khaya Bay, SE Laptev Sea. *Biogeochemistry* 8, 1865–1879.
- Kim, J.-H., Ludwig, W., Schouten, S., Kerhervé, P., Herfort, L., Bonnin, J., Sinninghe Damsté, J.S., 2007. Impact of flood events on the transport of terrestrial organic matter to the ocean: a study of the Têt River (SW France) using the BIT index. *Organic Geochemistry* 38, 1593–1606.
- Lincoln, S.A., Wai, B., Matthew, J.M., Church, J., Summons, R.E., DeLong, E.F., 2014. Planktonic Euryarchaeota are a significant source of archaeal tetraether lipids in the ocean. *Proceedings of the National Academy of Sciences USA* 111, 9858–9863.
- Lobb, J.M., Fitzner, H.P., Kattner, G., 2000. Biogeochemical characteristics of dissolved and particulate organic matter in Russian rivers entering the Arctic Ocean. *Geochimica et Cosmochimica Acta* 64, 2973–2983.
- McClymont, E.L., Ganeshram, R.S.S., Pichevin, L.E., Talbot, H., van Dongen, B., Thunell, R.C., Haywood, A.M., Singarayer, J.S., Valdes, P.J., 2012. Sea-surface temperature records of Termination 1 in the Gulf of California: challenges for seasonal and inter-annual analogues of tropical Pacific climate change. *Paleoceanography* 27, PA2202. <http://dx.doi.org/10.1029/2011PA022206>.
- Ouiris, G., Rohmer, M., 1982. Prokaryotic polyterpenes: phylogenetic precursors of sterols. *Current Topics in Membranes and Transport* 17, 153–182.
- Ouiris, G., Rohmer, M., Poralla, K., 1987. Prokaryotic hopanoids and other polyterpenoid sterol surrogates. *Annual Review of Microbiology* 41, 301–333.
- Peterse, F., Hopmans, E.C., Schouten, S., Mets, A., Rijpstra, W.I.C., Sinninghe Damsté, J.S., 2011. Identification and distribution of intact polar branched tetraether lipids in peat and soil. *Organic Geochemistry* 42, 1007–1015.
- Peterse, F., Vonk, J.E., Holmes, R.M., Giosan, L., Zimov, N., Eglinton, T.I., 2014. Branched glycerol dialkyl glycerol tetraethers in Arctic lake sediments: sources and implications for paleothermometry at high latitudes. *Journal of Geophysical Research – Biogeochemistry* 119, 1738–1754.
- Rethemeyer, J., Schubotz, F., Talbot, H.M., Cooke, M.P., Hinrichs, K.-U., Mollenhauer, G., 2010. Distribution of polar membrane lipids in permafrost soils and sediments of a small high Arctic catchment. *Organic Geochemistry* 41, 1130–1145.
- Rohmer, M., 1993. The biosynthesis of triterpenoids of the hopane series in the Eubacteria: a mine of new enzyme reactions. *Pure & Applied Chemistry* 65, 1293–1298.
- Sabine, C.L., Feely, R.A., Gruber, N., Key, R.M., Lee, K., Bullister, J.L., Wanninkhof, R., Wong, C.S., Wallace, D.W.R., Tilbrook, B., Millero, F.J., Peng, T.-H., Kozyr, A., Ono, T., Rios, A.F., 2004. The oceanic sink for anthropogenic CO_2 . *Science* 305, 367–371.
- Sáenz, J.P., Eglinton, T.I., Summons, R.E., 2011a. Abundance and structural diversity of bacteriohopanepolyols in suspended particulate matter along a river to ocean transect. *Organic Geochemistry* 42, 774–780.
- Sáenz, J.P., Wakeham, S.G., Eglinton, T.I., Summons, R.E., 2011b. New constraints on the provenance of hopanoids in the marine geologic record: bacteriohopanepolyols in marine suboxic and anoxic environments. *Organic Geochemistry* 42, 1351–1362.
- Sánchez-García, L., Alling, V., Pugach, S., Vonk, J., van Dongen, B.E., Humborg, C., Dudarev, O., Semiletov, I., Gustafsson, Ö., 2011. Inventories and behavior of particulate organic carbon in the Laptev and East Siberian seas. *Global Biogeochemical Cycles* 25, GB2007.
- Sánchez-García, L., Vonk, J.E., Charkin, A.N., Kosmach, D., Dudarev, O.V., Semiletov, I.P., Gustafsson, Ö., 2014. Characterisation of three regimes of collapsing Arctic ice complex deposits on the SE Laptev Sea coast using biomarkers and dual carbon isotopes. *Permafrost and Periglacial Processes* 25, 172–183.
- Schleper, C., Nicol, G.W., Robert, K.P., 2010. Ammonia-oxidising archaea-physiology, ecology and evolution. *Advances in Microbial Physiology*, vol. 57. Academic Press, pp. 1–41.
- Schouten, S., Pitcher, A., Hopmans, E.C., Villanueva, L., van Bleijswijk, J., Sinninghe Damsté, J.S., 2012. Intact polar and core glycerol dibiphytanyl glycerol tetraether lipids in the Arabian Sea oxygen minimum zone: I. Selective preservation and degradation in the water column and consequences for the TEX_{86} . *Geochimica et Cosmochimica Acta* 98, 228–243.
- Schouten, S., Hopmans, E.C., Sinninghe Damsté, J.S., 2013a. The organic geochemistry of glycerol dialkyl glycerol tetraether lipids: a review. *Organic Geochemistry* 54, 19–61.
- Schouten, S., Hopmans, E.C., Rosell-Melé, A., Pearson, A., Adam, P., Bauersachs, T., Bard, E., Bernasconi, S.M., Bianchi, T.S., Brocks, J.J., Carlson, L.T., Castañeda, I.S., Derenne, S., Doğrul Selver, A., Dutta, K., Eglinton, T., Fosse, C., Galy, V., Grice, K., Hinrichs, K.-U., Huang, Y., Huguet, A., Huguet, C., Hurlley, S., Ingalls, A., Jia, G., Keely, B., Knappy, C., Kondo, M., Krishnan, S., Lincoln, S., Lipp, J., Mangelsdorf, K., Martínez-García, A., Ménot, G., Mets, A., Mollenhauer, G., Ohkouchi, N., Ossebaer, J., Pagani, M., Pancost, R.D., Pearson, E.J., Peterse, F., Reichart, G.-J., Schaeffer, P., Schmitt, G., Schwark, L., Shah, S.R., Smith, R.W., Smittenberg, R.H., Summons, R.E., Takano, Y., Talbot, H.M., Taylor, K.W.R., Tarozo, R., Uchida, M., van Dongen, B.E., Van Mooy, B.A.S., Wang, J., Warren, C., Weijers, J.W.H., Werne, J.P., Woltering, M., Xie, S., Yamamoto, M., Yang, H., Zhang, C.L., Zhang, Y., Zhao, M., Sinninghe Damsté, J.S., 2013b. An interlaboratory study of TEX_{86} and BIT analysis of sediments, extracts, and standard mixtures. *Geochemistry, Geophysics, Geosystems* 14, 5263–5285.
- Semiletov, I.P., Pipko, I.I., Repina, I., Shakhova, N.E., 2007. Carbonate chemistry dynamics and carbon dioxide fluxes across the atmosphere–ice–water interfaces in the Arctic Ocean: Pacific sector of the Arctic. *Journal of Marine Systems* 66, 204–226.
- Semiletov, I., Gustafsson, Ö., 2009. East Siberian Shelf study alleviates scarcity of observations. *Eos, Transactions American Geophysical Union* 90, 145–146.
- Semiletov, I.P., Shakhova, N.E., Sergienko, V.I., Pipko, I.I., Dudarev, O.V., 2012. On carbon transport and fate in the East Siberian Arctic land–shelf–atmosphere system. *Environmental Research Letters* 7, 015201.
- Semiletov, I.P., Shakhova, N.E., Pipko, I.I., Pugach, S.P., Charkin, A.N., Dudarev, O.V., Kosmach, D.A., Nishino, S., 2013. Space–time dynamics of carbon and environmental parameters related to carbon dioxide emissions in the Buor-Khaya Bay and adjacent part of the Laptev Sea. *Biogeochemistry* 10, 5977–5996.
- Shakhova, N., Semiletov, I., 2007. Methane release and coastal environment in the East Siberian Arctic shelf. *Journal of Marine Systems* 66, 227–243.
- Shakhova, N., Semiletov, I., Salyuk, A., Yusupov, V., Kosmach, D., Gustafsson, Ö., 2010. Extensive methane venting to the atmosphere from sediments of the East Siberian Arctic Shelf. *Science* 327, 1246–1250.
- Shakhova, N., Semiletov, I., Leifer, I., Sergienko, V., Salyuk, A., Kosmach, D., Chernikh, D., Stubbs, C., Nicolsky, D., Tumskey, V., Gustafsson, Ö., 2014. Ebullition and storm-induced methane release from the East Siberian Arctic Shelf. *Nature Geoscience* 7, 64–70.
- Sinninghe Damsté, J.S., Hopmans, E.C., Pancost, R.D., Schouten, S., Genevasen, J.A.J., 2000. Newly discovered non-isoprenoid glycerol dialkyl glycerol tetraether lipids in sediments. *Chemical Communications* 17, 1683–1684.
- Sinninghe Damsté, J.S., Schouten, S., Hopmans, E.C., Van Duin, C.T., Genevasen, J.A.J., 2002. Crenarchaeol: the characteristic core glycerol dibiphytanyl glycerol tetraether membrane lipid of cosmopolitan pelagic crenarchaeota. *Journal of Lipid Research* 43, 1641–1651.
- Sinninghe Damsté, J.S., Ossebaer, J., Abbas, B., Schouten, S., Verschuren, D., 2009. Fluxes and distribution of tetraether lipids in an equatorial African lake: Constraints on the application of the TEX_{86} palaeothermometer and BIT index in lacustrine settings. *Geochimica et Cosmochimica Acta* 73, 4232–4249.

- Smith, R.W., Bianchi, T.S., Savage, C., 2010. Comparison of lignin phenols and branched/isoprenoid tetraethers (BIT index) as indices of terrestrial organic matter in Doubtful Sound, Fiordland, New Zealand. *Organic Geochemistry* 41, 281–290.
- Smith, R.W., Bianchi, T.S., Li, X., 2012. A re-evaluation of the use of branched GDGTs as terrestrial biomarkers: implications for the BIT Index. *Geochimica et Cosmochimica Acta* 80, 14–29.
- Stein, R., MacDonald, R.W., 2004. *The Organic Carbon Cycle in the Arctic Ocean*. Springer, Berlin.
- Strong, D.J., Flecker, R., Valdes, P.J., Wilkinson, I.P., Rees, J.G., Zong, Y.Q., Lloyd, J.M., Garrett, E., Pancost, R.D., 2012. Organic matter distribution in the modern sediments of the Pearl River Estuary. *Organic Geochemistry* 49, 68–82.
- Talbot, H.M., Summons, R., Jahnke, L., Farrimond, P., 2003. Characteristic fragmentation of bacteriohopanepolyols during atmospheric pressure chemical ionisation liquid chromatography/ion trap mass spectrometry. *Rapid Communications in Mass Spectrometry* 17, 2788–2796.
- Talbot, H.M., Farrimond, P., 2007. Bacterial populations recorded in diverse sedimentary bioproduct distributions. *Organic Geochemistry* 38, 1212–1225.
- Tarnocai, C., Canadell, J.G., Schuur, E.A.G., Kuhry, P., Mazhitova, G., Zimov, S., 2009. Soil organic carbon pools in the northern circumpolar permafrost region. *Global Biogeochemical Cycles* 23, GB2023.
- Taylor, K.A., Harvey, R.H., 2011. Bacterial hopanoids as tracers of organic carbon sources and processing across the western Arctic continental shelf. *Organic Geochemistry* 42, 487–497.
- Tesi, T., Semiletov, I., Hugelius, G., Dudarev, O., Kuhry, P., Gustafsson, Ö., 2014. Composition and fate of terrigenous organic matter along the Arctic land–ocean continuum in East Siberia: insights from biomarkers and carbon isotopes. 133, 235–256.
- The Royal Society, 2005. *Ocean Acidification due to Increasing Atmospheric Carbon Dioxide*. Policy document 12/05. The Royal Society, London.
- Tierney, J.E., Russell, J.M., 2009. Distributions of branched GDGTs in a tropical lake system: implications for lacustrine application of the MBT/CBT paleoproxy. *Organic Geochemistry* 40, 1032–1036.
- Tierney, J.E., Schouten, S., Pitcher, A., Hopmans, E.C., Sinninghe Damsté, J.S., 2012. Core and intact polar glycerol dialkyl glycerol tetraethers (GDGTs) in Sand Pond, Warwick, Rhode Island (USA): insights into the origin of lacustrine GDGTs. *Geochimica et Cosmochimica Acta* 77, 561–581.
- Trenberth, K.E., Jones, P.D., Ambenje, P., Bojariu, R., Easterling, D., Klein Tank, A., Parker, D., Rahimzadeh, F., Renwick, J.A., Rusticucci, M., Soden, B., Zha, P., 2007. Observations: surface and atmospheric climate change. In: Solomon, S., Qin, D., Manning, M., Chen, Z., Marquis, M., Averyt, K.B., Tignor, M., Miller, H.L. (Eds.), *Climate Change 2007: The Physical Science Basis*. Contribution of Working Group I to the Fourth Assessment Report of the Intergovernmental Panel on Climate Change, Cambridge, UK and New York, NY, USA.
- Uhlířová, E., Šantrůčková, H., Davidov, S.P., 2007. Quality and potential biodegradability of soil organic matter preserved in permafrost of Siberian tussock tundra. *Soil Biology and Biochemistry* 39, 1978–1989.
- van Dongen, B.E., Irene, C., Rijpstra W., Philippart, C.J.M., de Leeuw, J.W., Sinninghe Damsté, J.S., 2000. Biomarkers in upper Holocene Eastern North Sea and Wadden Sea sediments. *Organic Geochemistry* 31, 1533–1543.
- van Dongen, B.E., Talbot, H.M., Schouten, S., Pearson, P.N., Pancost, R.D., 2006. Well preserved Palaeogene and Cretaceous biomarkers from the Kilwa area, Tanzania. *Organic Geochemistry* 37, 539–557.
- van Dongen, B.E., Semiletov, I., Weijers, J.W.H., Gustafsson, Ö., 2008a. Contrasting lipid biomarker composition of terrestrial organic matter exported from across the Eurasian Arctic by the five great Russian Arctic rivers. *Global Biogeochemical Cycles* 22, GB1011.
- van Dongen, B.E., Zencak, Z., Gustafsson, Ö., 2008b. Differential transport and degradation of bulk organic carbon and specific terrestrial biomarkers in the surface waters of a sub-arctic brackish bay mixing zone. *Marine Chemistry* 112, 203–214.
- van Winden, J.F., Talbot, H.M., Kip, N., Reichart, G.-J., Pol, A., McNamara, N.P., Jetten, M.S.M., Op den Camp, H.J.M., Sinninghe Damsté, J.S., 2012. Bacteriohopanepolyol signatures as markers for methanotrophic bacteria in peat moss. *Geochimica et Cosmochimica Acta* 77, 52–61.
- Vonk, J.E., van Dongen, B.E., Gustafsson, Ö., 2008. Lipid biomarker investigation of the origin and diagenetic state of sub-arctic terrestrial organic matter presently exported into the northern Bothnian Bay. *Marine Chemistry* 112, 1–10.
- Vonk, J.E., Sánchez-García, L., Semiletov, I.P., Dudarev, O.V., Eglinton, T.I., Andersson, A., Gustafsson, Ö., 2010. Molecular and radiocarbon constraints on sources and degradation of terrestrial organic carbon along the Kolyma paleoriver transect, East Siberian Sea. *Biogeosciences* 7, 3153–3166.
- Vonk, J.E., Sanchez-Garcia, L., van Dongen, B.E., Alling, V., Kosmach, D., Charkin, A., Semiletov, I.P., Dudarev, O.V., Shakhova, N., Roos, P., Eglinton, T.I., Andersson, A., Gustafsson, Ö., 2012. Activation of old carbon by erosion of coastal and subsea permafrost in Arctic Siberia. *Nature* 489, 137–140.
- Vonk, J.E., Gustafsson, Ö., 2013. Permafrost-carbon complexities. *Nature Geoscience* 6, 675–676.
- Walsh, M.E., Ingalls, A.E., Keil, R.G., 2008. Sources and transport of terrestrial organic matter in Vancouver Island fjords and the Vancouver–Washington Margin: a multiproxy approach using $\delta^{13}\text{C}_{\text{org}}$, lignin phenols, and the ether lipid BIT index. *Limnology and Oceanography* 53, 1054–1063.
- Weijers, J.W.H., Schouten, S., Spaargaren, O.C., Sinninghe Damsté, J.S., 2006. Occurrence and distribution of tetraether membrane lipids in soils: implications for the use of the TEX₈₆ proxy and the BIT index. *Organic Geochemistry* 37, 1680–1693.
- Weijers, J.W.H., Schouten, S., van den Donker, J.C., Hopmans, E.C., Sinninghe Damsté, J.S., 2007. Environmental controls on bacterial tetraether membrane lipid distribution in soils. *Geochimica et Cosmochimica Acta* 71, 703–713.
- Weijers, J.W.H., Blaga, C.I., Werne, J.P., Sinninghe Damsté, J.S., 2009. Microbial membrane lipids in lake sediments as a paleothermometer. *PAGES news* 17.
- Weijers, J.W.H., Bernhardt, B., Peterse, F., Werne, J.P., Dungait, J.A.J., Schouten, S., Sinninghe Damsté, J.S., 2011. Absence of seasonal patterns in MBT-CBT indices in mid-latitude soils. *Geochimica et Cosmochimica Acta* 75, 3179–3190.
- Xu, Y., Cooke, M.P., Talbot, H.M., Simpson, M.J., 2009. Bacteriohopanepolyol signatures of bacterial populations in Western Canadian soils. *Organic Geochemistry* 40, 79–86.
- Zell, C., Kim, J.-H., Hollander, D., Lorenzoni, L., Baker, P., Silva, C.G., Nittrouer, C., Sinninghe, Damsté, J.S., 2014. Sources and distributions of branched and isoprenoid tetraether lipids on the Amazon shelf and fan: implications for the use of GDGT-based proxies in marine sediments. *Geochimica et Cosmochimica Acta* 139, 293–312.
- Zell, C., Kim, J.-H., Moreira-Turcq, P., Abril, G., Hopmans, E.C., Bonnet, M.P., Lima Sobrinho, R., Sinninghe Damsté, J.S., 2013. Disentangling the origins of branched tetraether lipids and crenarchaeol in the lower Amazon River: implications for GDGT-based proxies. *Limnology and Oceanography* 58, 343–353.
- Zhu, C., Talbot, H.M., Wagner, T., Pan, J.-M., Pancost, R.D., 2011a. Distribution of hopanoids along a land to sea transect: implications for microbial ecology and the use of hopanoids in environmental studies. *Limnology and Oceanography* 56, 1850–1865.
- Zhu, C., Weijers, J.W.H., Wagner, T., Pan, J.-M., Chen, J.-F., Pancost, R.D., 2011b. Sources and distributions of tetraether lipids in surface sediments across a large river-dominated continental margin. *Organic Geochemistry* 42, 376–386.
- Zhu, C., Wagner, T., Talbot, H.M., Weijers, J.W.H., Pan, J.-M., Pancost, R.D., 2013. Mechanistic controls on diverse fates of terrestrial organic components in the East China Sea. *Geochimica et Cosmochimica Acta* 117, 129–143.
- Zwiers, F.W., 2002. Climate change: the 20-year forecast. *Nature* 416, 690–691.